E-ISSN 2586-9027
Homepage : https://tci-thaijo.org/index.php/SciTechAsia
Science & Technology Asia
Vol.31 No.3 July - September 2026
Page: [309-320]
Original research article

A Proteomic Dataset of HepG2 Cellular Responses to Cycloheximide-Induced Translational Arrest

Thanawan Soimanee[1], Narumon Phaonakrop[2], Sittiruk Roytrakul[2], Chareeporn Akekawatchai[3,4,*]

[1]*Graduate Program in Biomedical Sciences, Faculty of Allied Health Sciences, Thammasat University, Pathum Thani 12120, Thailand*
[2]*National Center for Genetic Engineering and Biotechnology, National Science and Technology Development Agency, Pathum Thani 12120, Thailand*
[3]*Department of Medical Technology, Faculty of Allied Health Sciences, Thammasat University, Pathum Thani 12120, Thailand*
[4]*Research Unit in Diagnostic Molecular Biology of Chronic Diseases Related to Cancer, Thammasat University, Pathum Thani 12120, Thailand*

Received 13 June 2026; Received in revised form 19 July 2026
Accepted 31 July 2026; Available online 30 September 2026

ABSTRACT

Cycloheximide (CHX), a potent translational inhibitor, is widely used in cellular assays requiring translational blockade. Due to limited characterization of CHX-exposed cellular models, this study investigated the molecular and cellular effects of CHX in human hepatoma HepG2 cells. Cells were treated with various CHX concentrations for early (1 and 3 hours) and prolonged (18 and 24 hours) periods and evaluated for cellular responses. MTT assays showed no significant viability changes during early exposure, whereas prolonged treatment with 25 and 50 uM CHX reduced viability by approximately 30%. Sustained CHX exposure induced S-phase cell cycle arrest with minimal apoptosis (approximately 10%). LC-MS/MS analysis identified 19,482 differentially expressed proteins (DEPs), while PLS-DA revealed clear separation between untreated and CHX-treated HepG2 proteomes across time points. Volcano plot analysis identified the five most altered proteins at each time point, representing diverse cellular compartments and biological functions. STITCH network analysis further identified three interactome clusters associated with CHX responses: calcium-mediated survival signaling, xenobiotic detoxification, and ubiquitin-proteasome degradation. This characterized CHX-exposed HepG2 model provides a useful methodological reference for bioassays requiring translational stress.

Keywords: Cell cycle arrest; Cycloheximide; HepG2; Proteomics; Translational arrest

***Corresponding author:** cakekawatchai@gmail.com doi.org/10.70730/sta.v31i3.266187

1. Introduction

Cycloheximide (CHX), an antifungal agent isolated from *Streptomyces griseus*, is widely recognized as a potent inhibitor of eukaryotic protein synthesis, specifically blocking the translocation step during translational elongation [1]. Due to its ability to arrest *de novo* protein production, CHX serves as a foundational biochemical tool for determining protein half-lives and investigating translational control mechanisms [1-3]. It is also extensively utilized in various cellular assays, such as halting ribosomes for genome-wide profiling (Ribo-seq) [4] and sensitizing cancer cells to tumor necrosis factor receptor 1 (TNFR1)-induced apoptosis by depleting short-lived anti-apoptotic proteins [5]. Despite its widespread use as a specific translational inhibitor, recent evidence demonstrates that CHX does not merely suppress translation; rather, it actively triggers ribotoxic and endoplasmic reticulum stress, leading to complex cytostatic and morphological changes [6, 7]. Thus, the underlying molecular and cellular responses to CHX exposure require further clarification.

In hepatic research, the human hepatoma HepG2 cell line serves as an *in vitro* model for diverse biochemical studies, including oncogenesis and liver cytotoxicity [8]. Since its establishment in the 1970s, the cell line has been utilized in over 34,000 biomedical studies [8]. As a protein synthesis inhibitor, CHX is utilized to halt *de novo* protein synthesis, allowing researchers to measure protein stability [9]. However, CHX also induces complex alterations in cell survival and death pathways in HepG2 cells. While it exhibits a cytoprotective effect during serum withdrawal stress [10], CHX can sensitize cells to apoptosis when combined with death-inducing ligand tumor necrosis factor-alpha (TNF-α) [11]. Furthermore, prolonged CHX exposure causes general cell death rather than simply inhibiting translation [12]. Thus, it is essential to evaluate both the translation-inhibitory and the cytotoxic or cytoprotective effect in cellular models. Although proteome-wide mapping has identified short-lived proteins (half-life ≤ 8 hours) in CHX-treated human osteosarcoma and embryonic kidney cells [3], a comprehensive characterization of the underlying proteomic profiles responsible for CHX-mediated molecular and cellular alterations in HepG2 cells remains to be defined.

Therefore, this study utilizes high-throughput liquid chromatography-tandem mass spectrometry (LC-MS/MS) coupled with chemical-protein interaction network analysis to describe the molecular and cellular alterations in CHX-treated HepG2 cells. By linking protein profiles with observed phenotypes, our findings provide a critical methodological framework and biological reference for interpreting protein translation assays and cellular stress responses in hepatic cell models.

2. Materials and Methods

2.1 Cell lines, maintenance, and reagents

The human hepatocellular carcinoma cell line HepG2 was obtained from the American Type Culture Collection (ATCC HB-8065, Manassas, VA, USA). Cells were maintained in complete low-glucose Dulbecco's Modified Eagle Medium (DMEM) supplemented with 10% (v/v) heat-inactivated fetal bovine serum, 1M HEPES, and 1% penicillin/streptomycin (all from GibcoBRL, NY, USA), at 37 °C in a humidified atmosphere containing 5% CO_2. CHX was purchased from Sigma-Aldrich (Cat no. 01810, St. Louis, MO, USA) and prepared as a stock solution at a concentration of 1 mM in deionized water.

2.2 Cell viability assessment by 3-(4,5-Dimethylthiazol-2-yl)-2,5-Diphenyltetrazolium bromide assay

Cells were seeded into 96-well plates at a density of 2×10^5 cells/well and cultured overnight. Following CHX treatment for the indicated time points, 50 μL of 0.5 mg/mL 3-(4,5-dimethylthiazol-2-yl)-2,5-diphenyltetrazolium bromide (MTT) in phosphate buffer saline (PBS) was added to each well. After a 3-hour incubation, the medium was aspirated and the formed formazan crystals were dissolved in 150 μL of DMSO/well. Absorbance was measured at 570 nm using a microplate reader (BioTek Instruments, Winooski, VT, USA) [13]. Cell viability inhibition was calculated as a percentage relative to untreated control cultures.

2.3 Cell cycle and apoptosis analysis by flow cytometry

Cells were cultured in 6-well plate at a density of 5×10^5 cells/well overnight. Following CHX treatment for the specific time points, cells were trypsinized and harvested. For cell cycle and apoptosis analyses, cells were stained using the Muse® Cell Cycle Assay Kit and MUSE™ Annexin V & Dead Cell kit (Both from Merk Millipore Co., Darmstadt, Germany), respectively, according to the manufacturer's instructions. Quantitative analysis was performed using a Muse™ cell analyzer (Merk Millipore Co., Darmstadt, Germany).

2.4 Proteomic and Bioinformatic analysis

Cells were seeded in 6-well plates at a density of 1×10^6 cells/well and cultured overnight. At specific time points of CHX treatment, the culture medium was removed, and the cells were washed once with cold PBS. Cells were harvested by scraping in 250 µL of ice-cold RIPA buffer (Sigma-Aldrich) supplemented with 1X protease inhibitor cocktail (Roche, Mannheim, Germany), 2 mM sodium orthovanadate, 10 mM sodium fluoride, 2 mM phenylmethysulphonyl fluoride, and phosphatase inhibitor cocktail 2 and 3 (Sigma-Aldrich). Cell lysates were immediately collected and stored in -80°C until further LC-MS/MS analysis.

Shotgun proteomic analysis was performed as previously described [14]. Briefly, total protein was quantified via the Lowry method [15]; subsequently, 50 μg of total protein per sample underwent standard reduction, alkylation, and in-solution tryptic digestion. Peptides were fractionated in technical triplicate using an Ultimate 300 Nano LC System on an Acclaim PepMap RSLC C18 column (Thermo Fisher Scientific, USA) with a 30-min linear gradient (5-55% acetonitrile). Mass spectrometry was performed on a ZenoTOF 7600 (SCIEX, USA) in positive ion, top 50 data-independent acquisition (DIA) mode with the Zeno trap enabled. Label-free quantification was executed in Max-Quant (v2.5.0.0) (Max-Planck Institute for Biochemistry) using the Andromeda engine against UniProt *Homo sapiens* database (downloaded on 28 March 2025) [16] and contaminant database (trypsin digestion, ≤ 2 missed cleavages, 0.6 Da tolerance, fixed cysteine carbamidomethylation, variable methionine oxidation/N-terminal acetylation with ≤ 5 modifications, 1% FDR). Targeted identification matched data against a custom peptide database. Downstream filtering, $\log_2$-transformation, zero-imputation, and unpaired t-tests were performed in Perseus (v1.6.6.0) [16], excluding non-UPS1 proteins. Intensity values of the MS/MS spectra were analyzed using partial least squares-discriminant analysis (PLS-DA) model (FDR < 0.05) and Volcano plot analysis using web-based tool MetaboAnalyst version 6.0 (metaboanalyst.ca/) [17]. Molecular function and subcellular distribution of identified proteins were obtained from UniProt database (uniprot.org/). A chemical-protein interaction network was constructed using the STITCH 5.0 database (stitch.embl.de/).

2.6 Statistical analysis

Data were analyzed by a two-way ANOVA followed by a Dunnett's post hoc test using GraphPad Prism 9.5.1 (GraphPad software, San Diego, CA, USA). Statistical significance was defined as $P < 0.05$.

3. Results and Discussion

3.1 Cellular responses to CHX treatment

Previous studies have used CHX at concentrations ranging from 25 to 50 μM to block translation and sensitize hepatic cells to death-receptor-mediated apoptosis [11, 18]. To characterize the cellular response and map proteomic changes, HepG2 cells in serum-free medium were exposed to CHX (1, 12.5, 25, 50, and 100 μM) for 1, 3, 18, and 24 hours, in parallel with untreated controls. MTT assay results (Figs. 1A and B) showed no significant changes in OD values across all tested concentrations at 3 hours but revealed a significant decrease by 24 hours ($P \leq 0.001$ and $P \leq 0.0001$). These findings were consistent with morphological changes observed in cultures treated with 50 μM CHX at 1, 3, and 18 hours compared with untreated cells (Fig. 1C). Notably, after 24 hours, CHX-treated cultures lost almost all cells due to detachment from the surface (Data not shown). Although 25-50 μM CHX is frequently used to pretreat cells prior to inducing cell death [11, 18], our results strongly indicated that while 3-hour exposure reduced cell viability by less than 10%, a prolonged 24-hour treatment significantly reduced viability to approximately 30%. Additionally, cell cycle and apoptosis analyses indicated significant S-phase cell cycle arrest ($P < 0.0001$) and low levels of apoptosis (approximately 10%) ($P < 0.01$) after 24 hours of 50 μM CHX treatment. These results suggest that CHX exerts a cytostatic effect, possibly due to the depletion of short-lived proteins involved in the cell cycle [3].

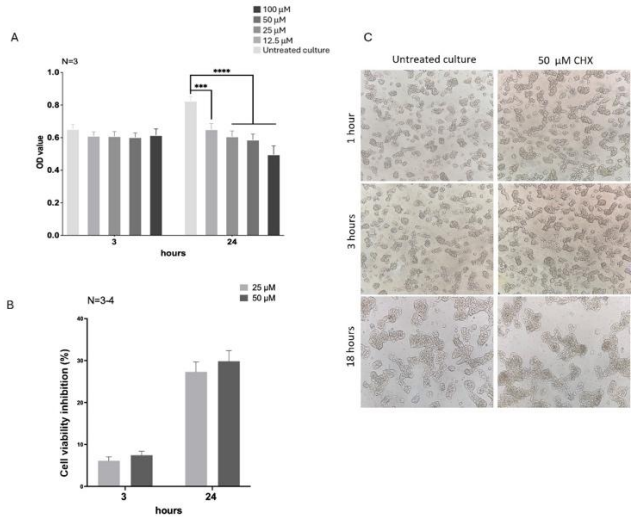


Fig. 1. CHX treatment decreased HepG2 cell viability. (A) OD values of untreated controls and cultures treated with 12.5, 25, 50 and 100 μM CHX. (B) Percent inhibition of cell viability relative to untreated controls following CHX-treated cultures (25 and 50 μM) for 3 and 24 hours. (C) Morphological alterations in HepG2 cells under light microscopy at 10x magnification following 24-hour exposure to 50 μM CHX. Data are represented as the mean ± S.E.M from N = 3 (A) and N = 3-4 (B) independent experiments, each performed in five technical replicates. ***, $P < 0.001$, ****, $P < 0.0001$. Abbreviation: CHX, cycloheximide.

However, at the tested doses and time points, it is likely that CHX did not directly induce apoptosis in HepG2 cells. Rather, CHX may deplete anti-apoptotic proteins, thereby sensitizing the cells to apoptosis induced by death inducers, including the death ligand TNF-α [5, 11, 18]. Collectively, our HepG2 model demonstrated that CHX concentrations (25 and 50 μM) reduced cell viability via cytostasis, possibly without directly inducing apoptosis during prolonged treatment. Given that CHX affects proteins with an 8-hour half-life, as shown in the previous study [3], our subsequent proteomic analysis was conducted on cultures treated with 50 uMCHX at early time points (1 and 3 hours) and at prolonged time points (18 and 24 hours).

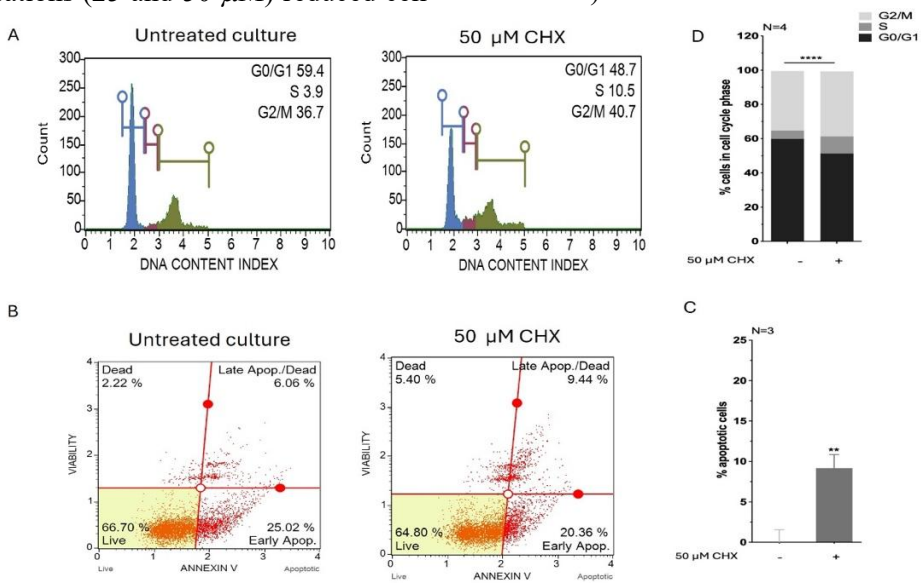


Fig. 2. CHX treatment induced S-phase cell cycle arrest in HepG2 cells, accompanied by low levels of apoptosis. (A) Flow cytometric analysis of DNA-stained cells showing cell cycle distribution in untreated and 50 μM CHX-treated cultures at 24 hours. (B) Annexin V-7AAD dot plots showing apoptotic cell populations in untreated and 50 μM CHX-treated cultures at 24 hours. (C and D) Bar graphs quantifying the percentages of cells in each cell cycle phase and apoptotic cell percentage, respectively. Data are presented as the mean ± S.E.M. from N=3 (D) and N = 3 (C) independent experiments, with technical duplicates.**, $P < 0.01$ and ****, $P < 0.0001$. Abbreviation: CHX, cycloheximide.

3.2 Proteomic profiling in response to CHX

Shotgun proteomics were conducted to analyze protein expression profiles in the CHX-treated cells at the four time points. A total of 19,482 DEPs were identified. PLS-DA models demonstrated clear clustering between the proteome of untreated and CHX-treated HepG2 cultures across the time points (Fig. 3A). To narrow down the dataset and prioritize only the highly altered proteins, volcano plots indicated significant DEPs for each time point, with the top five upregulated ($\log_2$ FC < - 4.0, $P < 0.001$) and downregulated ($\log_2$ FC > 4.0, $P < 0.001$) proteins detailed in Fig. 3B. Table 1 lists the 20 most significant DEPs identified via volcano plot analysis, comprising 4 downregulated and 16 upregulated proteins. These proteins were primarily located in the cell membrane, nucleus, mitochondria, endoplasmic reticulum, cytoskeleton, cytoplasm, cell projection, and extracellular space. Their key cellular and molecular functions include cytoskeleton organization, DNA replication, transcription, signal transduction, protein modification, mitochondrial transport, metabolism, cell

cycle regulation, apoptosis, reproduction, immune activation, and spermatogenesis. During early CHX treatment (1 and 3 hours), analysis revealed the downregulation of SUN domain-containing protein 5 and the upregulation of nine DEPs: ATP-binding cassette sub-family B member 10, tumor necrosis factor ligand superfamily member 13B, formin-binding protein 4, olfactory receptor 2A4, guanylyl cyclase-activating protein 3, zinc finger MYND domain-containing protein 12, carboxypeptidase M, actin nucleation-promoting factor WASL, and Cytochrome c1. In contrast, the prolonged CHX treatment (18 and 24 hours) downregulated Schlafen family member 11, zinc finger protein 99, and histone H1.4, while inducing the expression of chromosome transmission fidelity protein 8 homolog, epoxide hydrolase 1, endogenous retrovirus group K member 7 Pol protein, protein mono-ADP-ribosyltransferase PARP8, gastrokine-1, regucalcin, and insulin-like growth factor-binding protein 6. The differential expression of these candidate proteins suggests their potential roles in mediating the early and late cellular responses to CHX in HepG2 cells.

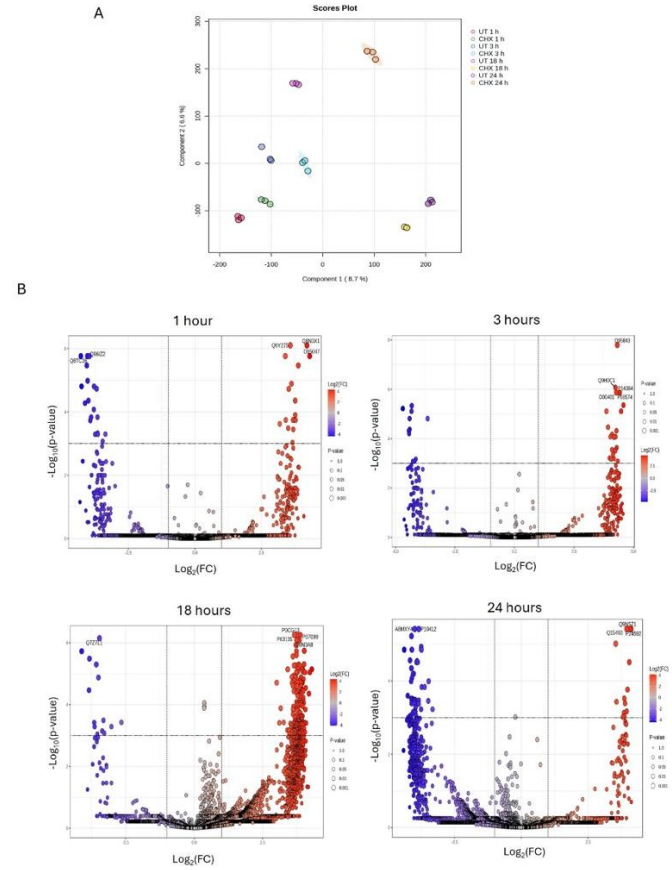


Fig. 3. DEPs identified by LC-MS/MS. (A) PLS-DA of 19,482 DEPs distinguishing between untreated and CHX-treated proteomes at 1, 3, 18 and 24 hours. (FDR < 0.05) (B) Volcano plots of all quantified proteins at each time point (X-axis: $\log_2$ fold change; Y-axis: $-\log_{10}$ FDR-adjusted *P*-value). Blue and red dots indicate significantly downregulated ($\log_2$ FC < - 4.0, $P < 0.001$) and upregulated ($\log_2$ FC > 4.0, $P < 0.001$) proteins in the CHX-treated proteome, respectively. The top five DEPs in each time point are labeled. Abbreviations: GeLC-MS/MS, Gel-enhanced liquid chromatography-tandem mass spectrometry; FDR, False discovery rate; FC, Fold change.

3.3 CHX-protein interaction networks by STITCH analysis

To explore the molecular functions of the 20 DEPs of interest identified by volcano plot analysis, their interactions with CHX were evaluated using the STITCH 5.0 database. As shown in Fig. 4, 13 out of the 20 candidate DEPs were included in the STITCH model. Out of these 13 proteins, seven did not interact with the CHX-protein network: zinc finger MYND-type containing 12 (ZMYND12), olfactory receptor family 2 subfamily A member 4 (OR2A4), gastrokine-1 (GKN1), zinc finger protein 99 (ZNF99), cytochrome c1(CYC1), carboxypeptidase M (CPM), Sad1, and UNC84 domain containing 5 (SUN5). In contrast, the remaining six candidate DEPs interacted with the CHX-protein network. These included the four upregulated DEPs: insulin-like growth factor binding protein 6 (IGFBP6), guanylate cyclase activator 1C (GUCA1C), regucalcin (RGN), and epoxide hydrolase 1 (EPHX1), as well as the two downregulated DEPs: Schlafen family member 11 (SLFN11) and histone cluster 1 H1e (HIST1H1E). Notably, GUCA1C was upregulated during the early stages of CHX treatment, whereas prolonged exposure upregulated IGFBP6, RGN, and EPHX1, and downregulated SLFN11 and HIST1H1E.

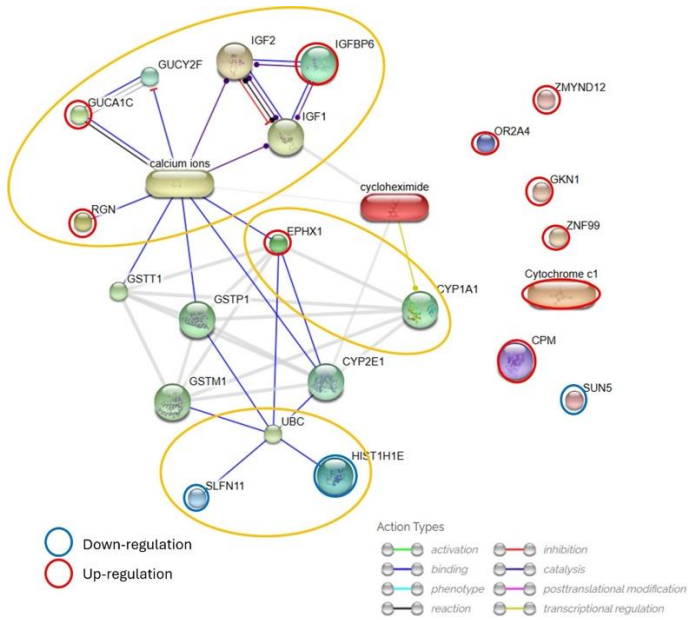


Fig. 4. Chemical-protein interaction network mapping CHX functional targets. The network details functional clusters in CHX-exposed HepG2 cells, comprising xenobiotic metabolism, the ubiquitin-proteasome (UPS) and calcium signaling pathways, which are highlighted by yellow ellipses. Network construction using the STITCH 5.0 database (accessed in June 2026) indicates interactions between CHX and six candidate proteins, including the down-regulated SLFN11 and HIST1H1E and the up-regulated RGN, GUCA1C, and IGFBP6. Seven other proteins are shown as non-interacting. Abbreviations: SLFN11, Schlafen family member 11; HIST1H1E, histone cluster 1; RGN, regucalcin; GUCA1C, guanylate cyclase activator 1C; IGFBP6, insulin-like growth factor binding protein 6; EPHX1, epoxide hydrolase 1.

This STITCH network analysis revealed three distinct interactome clusters responsible for CHX-mediated cellular changes, reflecting a temporal shift from early stress signaling to late-stage cellular adaptation. The first cluster is a calcium ion hub linking CHX exposure to the upregulation of RGN, IGFBP6, and

GUCA1C. Calcium is a crucial second messenger in the cellular stress response. The early upregulation of GUCA1C, an intracellular calcium-sensor protein [19], indicates an immediate activation of calcium-dependent signaling cascades. Conversely, the prolonged upregulation of the calcium-binding protein RGN and IGFBP6 suggests a late-stage compensatory mechanism. RGN is crucial for maintaining intracellular calcium homeostasis and exhibits potent anti-apoptotic properties under cellular stress [20, 21]. IGFBP6 is known to inhibit cell-cycle progression, promoting cytostasis [22, 23]. The concurrent upregulation of RGN and IGFBP6 strongly supports our flow cytometry data, which demonstrated CHX-induced cell-cycle arrest with minimal apoptosis in HepG2 cells during prolonged exposure. This suggests that the calcium ion hub plays a role in driving survival pathways during CHX-mediated severe cellular stress. The second cluster involves the interaction between CHX, cytochrome P4501A1 (CYP1A1), and upregulated EPHX1. Both are key enzymes in xenobiotic metabolism and cellular detoxification [24-26]. These findings suggest that HepG2 cells actively enhance their defense mechanisms against CHX toxicity during the later stages of treatment. Finally, the third cluster is anchored by Ubiquitin (UBC), which interacts with the downregulated SLFN11 and HIST1H1E during prolonged CHX exposure. UBC is encoded by a stress-inducible polyubiquitin gene that is upregulated to maintain ubiquitin homeostasis during proteotoxic stress [27, 28]. Functionally, SLFN11 is a potent, negative regulator of translation and DNA replication during cellular stress [29], while HIST1H1E, a linker histone, maintains highly condensed, inactive chromatin [30, 31]. A link between UBC and the downregulation of SLFN11 and HIST1H1E suggests that the ubiquitin-proteasome system actively targets unwanted or toxic proteins, including these two nuclear proteins, for degradation. Collectively, these dynamic signaling clusters sequentially mediated the CHX-induced cellular changes in HepG2 cells. Overall, these proteins tightly control cell fate (Table 3). While SLFN11, EPHX1, and IGFBP6 inhibit the cell cycle and trigger apoptosis, GCAP3 and, likely, RGN promote cell survival, and Histone H1.4 regulates both processes.

While this study provides mechanistic insights into the cellular response to translational inhibition, several methodological limitations must be acknowledged. First, 2D *in vitro* models lack physiological microenvironments, potentially altering the natural activation thresholds of the activation pathways. Second, although our dataset captures the proteomic landscape of translational arrest, it cannot perfectly distinguish whether CHX directly induces the modest apoptosis (approximately 10%) or only acts as a sensitizer. Clarifying this mechanism will require targeted evaluations of anti-apoptotic protein dynamics. Third, label-free quantitative proteomics captures static snapshots of net protein abundance. Thus, the observed up- or down-regulation reflects a comparative analysis relative to baseline expression at specific time points, rather than absolute measurements of continuous intracellular flux. Fourth, the lack of primary hepatocytes and altered survival pathways in immortalized cell lines may distort the exact timing of cellular collapse. Although dynamic tracking in 3D or *in vivo* models remains necessary to map real-time protein expression, the 2D CHX-exposed HepG2 model establishes a framework for studying cellular stress response to translational arrest. Importantly, this data set serves as a prolonged cautionary reference, warning that CHX exposure induces molecular alterations.

Table 1. Top five DEPs in CHX-treated HepG2 cells at 1, 3, 18, and 24 hours.

No.	Expression status	Accession no.	Protein	Fold change	Adjusted *P* value	Biological function	Subcellular distribution
1 hour of treatment							
1.	Down-regulated	Q8TC36	SUN domain-containing protein 5	0.0512	1.7336E-06	Spermatogenesis	Nucleus
2.	Down-regulated	Q9NRK6	ATP-binding cassette sub-family B member 10	0.0522	1.5656E-05	Mitochondrial transport	Mitochondria
3.	Up-regulated	Q9Y275	Tumor necrosis factor ligand superfamily member 13B	12.022	7.9881E-07	Immune system activation	Cell membrane
4.	Up-regulated	Q8N3X1	Formin-binding protein 4 (Formin-binding protein 30)	18.521	7.9881E-07	NA	NA
5.	Up-regulated	O95047	Olfactory receptor 2A4	19.903	1.7336E-06	Cytoskeleton/structure	Cell membrane
3 hours of treatment							
1.	Up-regulated	O95843	Guanylyl cyclase-activating protein 3	19.870	1.5998E-08	Signal transduction	Cell membrane
2.	Up-regulated	Q9H0C1	Zinc finger MYND domain-containing protein 12	18.811	8.5149E-07	Reproduction	Cell projection
3.	Up-regulated	P14384	Carboxypeptidase M	21.281	1.3655E-06	Protein modification	Cell membrane
4.	Up-regulated	O00401	Actin nucleation-promoting factor WASL	19.233	1.3655E-06	Cytoskeleton/structure	Cytoskeleton, nucleus, cytoplasm
5.	Up-regulated	P08574	Cytochrome c1	20.945	1.3655E-06	Metabolism	Mitochondria
18 hours of treatment							
1.	Down-regulated	Q7Z7L1	Schlafen family member 11	0.090	7.0356E-07	Cell cycle	Nucleus
2.	Up-regulated	P0CG13	Chromosome transmission fidelity protein 8 homolog	13.354	5.5552E-07	DNA replication	Nucleus
3.	Up-regulated	P07099	Epoxide hydrolase 1	14.621	5.5552E-07	Metabolism	Endoplasmic reticulum
4.	Up-regulated	P63135	Endogenous retrovirus group K member 7 Pol protein	12.644	5.5552E-07	DNA replication	Nucleus
5.	Up-regulated	Q8N3A8	Protein mono-ADP-ribosyltransferase PARP8	14.314	8.2438E-07	Protein modification	Endoplasmic reticulum, Nucleus, Cell membrane
24 hours of treatment							
1.	Down-regulated	A8MXY4	Zinc finger protein 99	0.062	3.7986E-06	Transcription	Nucleus
2.	Down-regulated	P10412	Histone H1.4	0.069	3.7986E-06	Transcription	Nucleus
3.	Up-regulated	Q9NS71	Gastrokine-1	16.674	3.7986E-06	Cell cycle	Extracellular region
4.	Up-regulated	Q15493	Regucalcin	15.359	3.7986E-06	Apoptosis	Cytoplasm
5.	Up-regulated	P24592	Insulin-like growth factor-binding protein 6	17.300	3.7986E-06	Signal transduction	Extracellular region

Note: Expression status is defined by a log2 fold change threshold of > 4.0 or < -4.0 and an adjusted *P* value of < 0.001. Accession no. corresponds to UniProtKB database identifiers. Annotations for biological function and subcellular distribution were extracted from the Gene Ontology database.

Table 2. Mass spectrometric characteristics of 20 DEPs in CHX-treated HepG2 cells at 1, 3, 18, and 24 hours.

No.	Accession no.	Peptide sequence	Protein	N: Q-value	N: Peptides	N: sequence coverage [%]	MH^+ (Da)
1 hour of treatment							
1.	Q8TC36	CKLLCQK	SUN domain-containing protein 5	0.9797	8	27.2	12017.80
2.	Q9NRK6	AFGKEMTEIEK	ATP-binding cassette sub-family B member 10	1.0024	31	37.7	43336.40
3.	Q9Y275	AELQGHHAEK	Tumor necrosis factor ligand superfamily member 13B	1.0120	7	24.2	8936.27
4.	Q8N3X1	EEEERWRR	Formin-binding protein 4 (Formin-binding protein 30)	1.0145	20	16.7	23351.50
5.	O95047	EFLLLGFPVGPR	Olfactory receptor 2A4	1.0400	6	17.7	6476.64
3 hours of treatment							
1.	O95843	AGLGKVK	Guanylyl cyclase-activating protein 3	1.0175	5	26.3	5909.63
2.	Q9H0C1	HEDAVPAALQSLR	Zinc finger MYND domain-containing protein 12	1.0635	8	24.9	13641.80
3.	P14384	DPEITNLINSTR	Carboxypeptidase M	1.0135	12	21.9	15972.70
4.	O00401	AALLDQIREGAQLKK	Actin nucleation-promoting factor WASL	1.0436	16	26.7	22125.50
5.	P08574	GAGLPGARAR	Cytochrome c1	1.0387	7	17.2	8826.30
18 hours of treatment							

1.	Q7Z7L1	CFYIFVKSWSSGPFPED RSVKPR	Schlafen family member 11	0.9996	31	37.4	46814.40
2.	P0CG13	DKILFKTRPKPIITSVPK	Chromosome transmission fidelity protein 8 homolog	1.0627	5	47.1	8331.97
3.	P07099	DKEETLPLEDGWWGPG TR	Epoxide hydrolase 1	1.0037	19	45.9	30421.80
4.	P63135	CTQQLRR	Endogenous retrovirus group K member 7 Pol protein	1.0002	30	20.0	45031.20
5.	Q8N3A8	ALDSITSIREMTQAPYL EIK	Protein mono-ADP-ribosyltransferase PARP8	1.0003	28	28.9	38748.50
24 hours of treatment							
1.	A8MXY4	AFKHFSALR	Zinc finger protein 99	1.0139	32	45.5	47464.00
2.	P10412	ALAAAGYDVEK	Histone H1.4	1.0398	17	63.9	19978.50
3.	Q9NS71	FGKNIANMCR	Gastrokine-1	1.0552	3	8.6	3749.40
4.	Q15493	EEQIPDGMCIDAEGK	Regucalcin	1.0127	10	35.1	13685.60
5.	P24592	APAVAEENPK	Insulin-like growth factor-binding protein 6	1.0062	9	36.2	14118.60

Note: N: Q-value: $-\log_{10}$-transformed FDR-adjusted *P*-value (> 1.30 and > 2.0 indicate < 5% and < 1% FDR, respectively). N: Peptides: Number of unique peptides matching the protein. N: Sequence coverage (%): Percentage of the protein sequence covered by identified peptides.

Table 3. Characteristics of 6 candidate proteins associated with CHX-protein interaction network.

No	Accession no.	Protein	STITCH pathways	Established biological function	Reference
1.	O95843	Guanylyl cyclase-activating protein 3	Calcium signaling	Loss of GCAP3 causes retinal cell apoptosis.	[32]
2.	Q7Z7L1	Schlafen family member 11	Ubiquitin-proteasome	SLFN11 induces cell cycle arrest and apoptosis.	[33, 34]
3.	P07099	Epoxide hydrolase 1	Xenobiotic metabolism	EPHX1 suppresses the cell cycle and induces apoptosis	[35] [36]
4.	P10412	Histone H1.4	Ubiquitin-proteasome	Histone H1 variant H1.4 regulates cell cycle and apoptosis	[37, 38]
5.	Q15493	Regucalcin	Calcium signaling	RGN regulates the cell cycle and death; directly prevents apoptosis	[20] [21]
6.	P24592	Insulin-like growth factor-binding protein 6	Calcium signaling	IGFBP6 inhibits the cell cycle and promotes apoptosis	[23, 24]

4. Conclusion

This study characterizes the temporal cellular and molecular dynamics of CHX-induced translational arrest. While acute treatment elicited no cellular change, prolonged CHX exposure resulted in decreased cell viability, S-phase cell cycle arrest, and minimal apoptosis. Network analysis of proteomic data revealed three molecular pathways responsible for these cellular responses, including xenobiotic detoxification, calcium-mediated survival signaling, and ubiquitin-proteasome degradation. This well-characterized CHX-exposed HepG2 model establishes a methodological reference for future bioassays investigating translational arrest.

Acknowledgements

The present study was supported by the Thammasat University Research Unit in Diagnostic Molecular Biology of Chronic Diseases Related to Cancer (DMB-CDC).

References

[1] Schneider-Poetsch T, Ju J, Eyler DE, Dang Y, Bhat S, Merrick WC, et al. Inhibition of eukaryotic translation elongation by cycloheximide and lactimidomycin. Nat Chem Biol. 2010;6(3):209-17.

[2] Kao SH, Wang WL, Chen CY, Chang YL, Wu YY, Wang YT, et al. Analysis of Protein Stability by the Cycloheximide Chase Assay. Bio Protoc. 2015;5(1).

[3] Li J, Cai Z, Vaites LP, Shen N, Mitchell DC, Huttlin EL, et al. Proteome-wide mapping of short-lived proteins in human cells. Mol Cell. 2021;81(22):4722-35 e5.

[4] Ingolia NT, Ghaemmaghami S, Newman JR, Weissman JS. Genome-wide analysis in vivo of translation with nucleotide resolution using ribosome profiling. Science. 2009;324(5924):218-23.

[5] Kreuz S, Siegmund D, Scheurich P, Wajant H. NF-kappaB inducers upregulate cFLIP, a cycloheximide-sensitive inhibitor of death

receptor signaling. Mol Cell Biol. 2001;21(12):3964-73.

[6] Ito K, Kiyosawa N, Kumagai K, Manabe S, Matsunuma N, Yamoto T. Molecular mechanism investigation of cycloheximide-induced hepatocyte apoptosis in rat livers by morphological and microarray analysis. Toxicology. 2006;219(1-3):175-86.

[7] Vind AC, Wu Z, Firdaus MJ, Snieckute G, Toh GA, Jessen M, et al. The ribotoxic stress response drives acute inflammation, cell death, and epidermal thickening in UV-irradiated skin in vivo. Mol Cell. 2024;84(24):4774-89 e9.

[8] Arzumanian VA, Kiseleva OI, Poverennaya EV. The Curious Case of the HepG2 Cell Line: 40 Years of Expertise. Int J Mol Sci. 2021;22(23).

[9] Li G, Qian Y, Chen Y, Cao M, Yang X, Kong D, et al. Wip1 contributes to the adaptation of HepG2 human liver cancer cells to stress hormone-induced DNA damage. Oncol Lett. 2023;25(1):31.

[10] Bai J, Cederbaum AI. Cycloheximide protects HepG2 cells from serum withdrawal-induced apoptosis by decreasing p53 and phosphorylated p53 levels. J Pharmacol Exp Ther. 2006;319(3):1435-43.

[11] Santiago-Lomeli M, Gomez-Quiroz LE, Ortiz-Ortega VM, Kershenobich D, Gutierrez-Ruiz MC. Differential effect of interleukin-10 on hepatocyte apoptosis. Life Sci. 2005;76(22):2569-79.

[12] Chan C, Martin P, Liptrott NJ, Siccardi M, Almond L, Owen A. Incompatibility of chemical protein synthesis inhibitors with accurate measurement of extended protein degradation rates. Pharmacol Res Perspect. 2017;5(5).

[13] Kumar P, Nagarajan A, Uchil PD. Analysis of Cell Viability by the MTT Assay. Cold Spring Harb Protoc. 2018;2018(6).

[14] Tarnathummanan C, Soimanee T, Khattiya J, Sretapunya W, Phaonakrop N, Roytrakul S, et al. Plasma proteomic profiles of patients with HIV infection and coinfection with hepatitis B/C virus undergoing anti-retroviral therapy. Biomed Rep. 2024;21(5):155.

[15] Lowry OH, Rosebrough NJ, Farr AL, Randall RJ. Protein measurement with the Folin phenol reagent. J Biol Chem. 1951;193(1):265-75.

[16] Tyanova S, Temu T, Cox J. The MaxQuant computational platform for mass spectrometry-based shotgun proteomics. Nat Protoc. 2016;11(12):2301-19.

[17] Pang Z, Zhou G, Ewald J, Chang L, Hacariz O, Basu N, et al. Using MetaboAnalyst 5.0 for LC-HRMS spectra processing, multi-omics integration and covariate adjustment of global metabolomics data. Nat Protoc. 2022;17(8):1735-61.

[18] Leist M, Gantner F, Bohlinger I, Germann PG, Tiegs G, Wendel A. Murine hepatocyte apoptosis induced in vitro and in vivo by TNF-alpha requires transcriptional arrest. J Immunol. 1994;153(4):1778-88.

[19] Palczewski K, Sokal I, Baehr W. Guanylate cyclase-activating proteins: structure, function, and diversity. Biochem Biophys Res Commun. 2004;322(4):1123-30.

[20] Yamaguchi M. The anti-apoptotic effect of regucalcin is mediated through multisignaling pathways. Apoptosis. 2013;18(10):1145-53.

[21] Marques R, Maia CJ, Vaz C, Correia S, Socorro S. The diverse roles of calcium-binding protein regucalcin in cell biology: from tissue expression and signalling to disease. Cell Mol Life Sci. 2014;71(1):93-111.

[22] Baxter RC. Signaling Pathways of the Insulin-like Growth Factor Binding Proteins. Endocr Rev. 2023;44(5):753-78.

[23] Lariz FJ, Hernandez S, Bautista-Tovar DC, Houston KD. IGFBP-6 regulates breast cancer cell cycle progression by promoting exit out of G1. J Biol Chem. 2026;302(2):111069.

[24] Pande M, Amos CI, Osterwisch DR, Chen J, Lynch PM, Broaddus R, et al. Genetic variation in genes for the xenobiotic-metabolizing enzymes CYP1A1, EPHX1, GSTM1, GSTT1, and GSTP1 and susceptibility to colorectal cancer in Lynch syndrome. Cancer Epidemiol Biomarkers Prev. 2008;17(9):2393-401.

[25] Thum T, Erpenbeck VJ, Moeller J, Hohlfeld JM, Krug N, Borlak J. Expression of xenobiotic metabolizing enzymes in different lung compartments of smokers and nonsmokers. Environ Health Perspect. 2006;114(11):1655-61.

[26] Walsh AA, Szklarz GD, Scott EE. Human cytochrome P450 1A1 structure and utility in understanding drug and xenobiotic metabolism. J Biol Chem. 2013;288(18):12932-43.

[27] Bianchi M, Crinelli R, Giacomini E, Carloni E, Radici L, Scarpa ES, et al. A negative feedback mechanism links UBC gene expression to ubiquitin levels by affecting RNA splicing rather than transcription. Sci Rep. 2019;9(1):18556.

[28] Kandel R, Jung J, Neal S. Proteotoxic stress and the ubiquitin proteasome system. Semin Cell Dev Biol. 2024;156:107-20.

[29] Murai J, Tang SW, Leo E, Baechler SA, Redon CE, Zhang H, et al. SLFN11 Blocks Stressed Replication Forks Independently of ATR. Mol Cell. 2018;69(3):371-84 e6.

[30] Hergeth SP, Schneider R. The H1 linker histones: multifunctional proteins beyond the nucleosomal core particle. EMBO Rep. 2015;16(11):1439-53.

[31] Zhao W, Zhang Y, Lv T, He J, Zhu B. A case report of a novel HIST1H1E mutation and a review of the bibliography to evaluate the genotype-phenotype correlations. Mol Genet Genomic Med. 2023;11(12):e2273.

[32] Morales-Camara S, Alexandre-Moreno S, Bonet-Fernandez JM, Atienzar-Aroca R, Aroca-Aguilar JD, Ferre-Fernandez JJ, et al. Role of GUCA1C in Primary Congenital Glaucoma and in the Retina: Functional Evaluation in Zebrafish. Genes (Basel). 2020;11(5).

[33] Jo U, Murai Y, Chakka S, Chen L, Cheng K, Murai J, et al. SLFN11 promotes CDT1 degradation by CUL4 in response to replicative DNA damage, while its absence leads to synthetic lethality with ATR/CHK1 inhibitors. Proc Natl Acad Sci U S A. 2021;118(6).

[34] Zoppoli G, Regairaz M, Leo E, Reinhold WC, Varma S, Ballestrero A, et al. Putative DNA/RNA helicase Schlafen-11 (SLFN11) sensitizes cancer cells to DNA-damaging agents. Proc Natl Acad Sci U S A. 2012;109(37):15030-5.

[35] Long X, Li Q, Zhi LJ, Li JM, Wang ZY. LINC00205 modulates the expression of EPHX1 through the inhibition of miR-184 in hepatocellular carcinoma as a ceRNA. J Cell Physiol. 2020;235(3):3013-21.

[36] Gautheron J, Morisseau C, Chung WK, Zammouri J, Auclair M, Baujat G, et al. EPHX1 mutations cause a lipoatrophic diabetes syndrome due to impaired epoxide hydrolysis and increased cellular senescence. Elife. 2021;10.

[37] Izquierdo-Bouldstridge A, Bustillos A, Bonet-Costa C, Aribau-Miralbes P, Garcia-Gomis D, Dabad M, et al. Histone H1 depletion triggers an interferon response in cancer cells via activation of heterochromatic repeats. Nucleic Acids Res. 2017;45(20):11622-42.

[38] Kratzmeier M, Albig W, Meergans T, Doenecke D. Changes in the protein pattern of H1 histones associated with apoptotic DNA fragmentation. Biochem J. 1999;337 (Pt 2)(Pt 2):319-27.